

Surface Modification of TiO₂-ZrO₂ Layers with Direct Diode Laser[†]

Nobuyuki ABE*, Masahiro TUKAMOTO**, Shinji FUKUHARA** and Junji MORIMOTO****

Abstract

Laser cladding technology has been used for erosion resistance, heat resistance and corrosion resistance. In the new solid cold spray process, the coating is formed by high-velocity particles impacting with the substrate to be coated. These particles bond mechanically with the substrate by way of plastic deformation only. Solid cold sprayed coatings have defects such as connected pores and poorly bonded lamellae which damage coating properties. In this research, a direct diode laser was utilized for laser treatments of cold sprayed composite coatings. The influence of laser power and scan speed, on the properties of the laser-treated layers was investigated. The laser treatment is the present subject of research in order to obtain denser coatings with good adhesion to the substrate. Therefore laser technology in combination with solid cold spraying broadens the area of applications for cold sprayed coatings.

KEY WORDS: (Direct diode laser)(Solid cold spray)(TiO₂-ZrO₂ coating)(Wear resistance)

1. Introduction

The cold spray process is a fairly recent process that shows promise as a complement to such well-established techniques as plasma spraying¹⁾ and high velocity oxy-fuel spraying²⁾. In the cold spray process³⁾, the coating is formed by high-velocity particles impacting with the substrate to be coated. The particles are accelerated by a jet of compressed air whose temperature is always lower than the melting temperature of the material being sprayed, and the coating is formed by particles in the solid state. These particles bond mechanically with the substrate by way of plastic deformation only⁴⁾. Solid cold sprayed coatings have defects such as connected pores and poorly bonded lamellae which damage coating properties. In this research, a direct diode laser was utilized for laser treatments of cold sprayed Zn-base composite coatings. The sprayed powders were Zn-Fe composite powder, ZrO₂ nanopowder, anatase TiO₂ nanopowder and WC-Co powder. The influence of the two most important laser-related variables, namely laser power and scan speed, on the properties of the laser-treated layers was investigated. Laser treatment is the present subject of research in order to obtain denser coatings with good adhesion to the substrate. Therefore laser technology in combination with solid cold spraying broadens the area of applications for cold sprayed coatings. The laser treated TiO₂-ZrO₂-WC-Co composite coatings showed high values of hardness from

1280 to 1490 VHN₅₀.

2. Experimental procedure

2.1 Solid cold spraying method and materials

For this experiment, the spraying conditions were compressed air jet pressure: 4~6 kg/cm², and spraying distance: 50~130mm. The sprayed powders were Zn-Fe composite powder, ZrO₂ nanopowder, anatase TiO₂ nanopowder and WC-12%Co powder. The SEM images of powder are shown in Fig.1. Zn-Fe alloy powder and ceramic powder were mechanically mixed with different ceramic content.

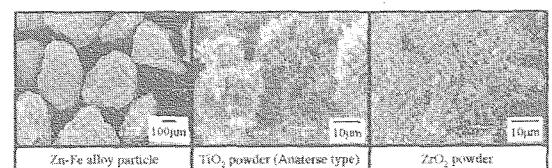


Fig.1 SEM micrographs of powder

Table 1 Zn-Fe composite powder

Composition (mass%)		Particle size distribution (%)				
Fe	Zn	>500 µm	~300 µm	~250 µm	~180 µm	<180 µm
Bal.	39.8	9.5	56.7	21.9	11.5	0.4

[†] Received on Nov.11, 2004

* Associate Professor

** Research Associate

*** Graduate Student, Kinki University

**** Professor, Kinki University

Transactions of JWRI is published by Joining and Welding Research Institute, Osaka University, Ibaraki, Osaka 567-0047, Japan

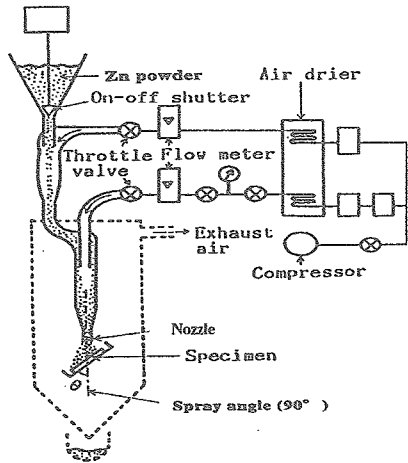


Fig.2 Schematic diagram of solid cold spray apparatus

The composition of the Zn-Fe spraying powder used in this study is shown in Table 1. Zn-Fe spraying powder has a hard core of Fe surrounded by the Zn layer. The base materials for the cold spraying were mild steel (SS400) and copper, which were polished before spraying. The substrates were 2mm thick steel (60×50mm), which was mechanically and chemically cleaned and then polished. The structure of the coating was examined by X-ray diffraction analysis. The microstructure of the cold sprayed coating was examined by scanning electron microscopy (SEM) and electron probe micro-analyzer (EPMA). The solid cold spray apparatus is illustrated in Fig.2. The mechanical properties of these coatings were evaluated by standard microhardness testing.

2.2 Laser irradiation to solid cold sprayed coating

Figure 3 shows a schematic drawing of the experimental apparatus. The copper plate was used as the substrate. The scan speed was varied between 2mm/sec and 16mm/sec. The laser beam power was varied between 100W and 200 W. The laser beam was focused on the surface of sprayed coating. Two laser irradiation patterns were used and are shown in Fig.3.

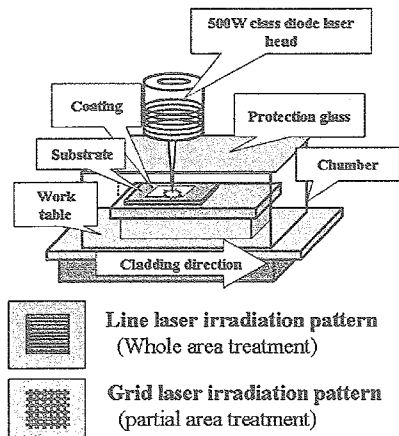


Fig.3 Schematic diagram of 500W class diode laser irradiation apparatus and irradiation pattern

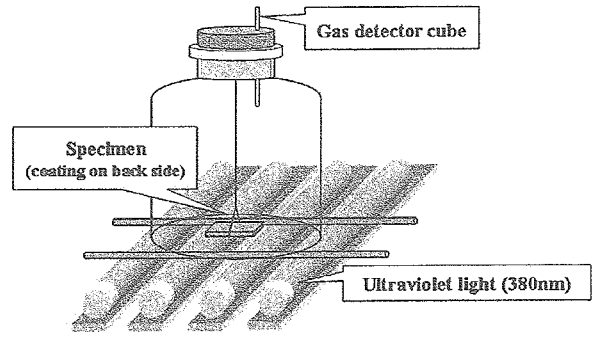


Fig.4 Schematic diagram of acetaldehyde gas decomposition test apparatus

2.3 Evaluation of photo-catalytic property of the coating

Acetaldehyde gas decomposition tests were carried out to evaluate the photo-catalytic property of the coating. The volume of the container was 2.1L. After the container was filled with acetaldehyde gas to 100 ppm, the ultraviolet lamps with a 360 nm wavelength were switched on. The experimental set-up is illustrated in Fig.4. The concentration of acetaldehyde gas was measured with a gas detector after a certain time interval.

3. Results and Discussion

3.1 Microstructure and properties of solid cold sprayed coatings

The results of SEM and EPMA images of the surface of solid cold sprayed TiO₂-Zn composite coating are shown in Fig.5. These images indicate that the surface of cold sprayed coatings consisted of mainly TiO₂, with small amount of Zn-Fe alloy dispersed particles. These specific properties determine the deformation share in the substrate and particle, as well as the degree of mechanical clamping and/or toothing, respectively, of coating and substrate. Figure 6 shows the surface of a laser-irradiated coating made at different laser powers, which mainly influenced remelting of particles. An increase in laser power improves surface roughness. The laser treated TiO₂-Zn coatings exhibit a high density and high bond strength.

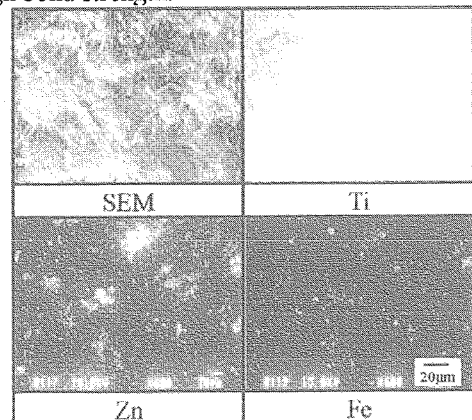


Fig.5 EPMA analysis of TiO₂-Zn sprayed coating (Composition rate,1:40)

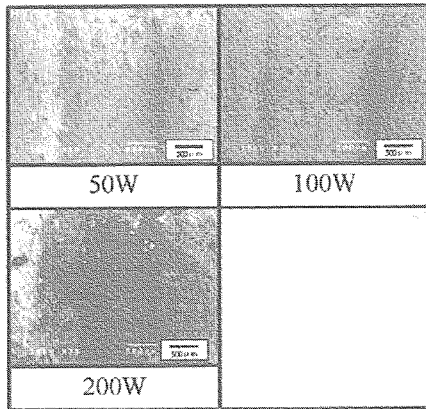


Fig.6 SEM images of TiO₂-Zn coating at different laser power (Scan speed of 8mm/sec)

3.2 Photo-catalytic properties of laser treated TiO₂-Zn coatings

In order to characterize the photo-catalytic property of the coating, decomposition tests of acetaldehyde gas were carried out. Figure 7 shows the results of acetaldehyde gas decomposition tests. This experiment was performed using cold spray TiO₂-Zn coatings and laser treated TiO₂-TiO₂-Zn coating. The photo-catalytic properties of the grid laser treated TiO₂-Zn coating were excellent, being equivalent to those of cold spray coatings. The characteristic decay time of line laser treated TiO₂-Zn coatings was worse than coatings without laser treatment. It is revealed that phase composition of the TiO₂-Zn composite coating is similar to that of starting powders. Figure 8 shows the XRD patterns of the line laser treated TiO₂-Zn composite coatings and grid laser treated TiO₂-Zn composite coatings. The anatase phases of TiO₂ remained in the grid laser treated coatings, and part of the anatase phases of TiO₂ has transformed into rutile phases by laser treatment.

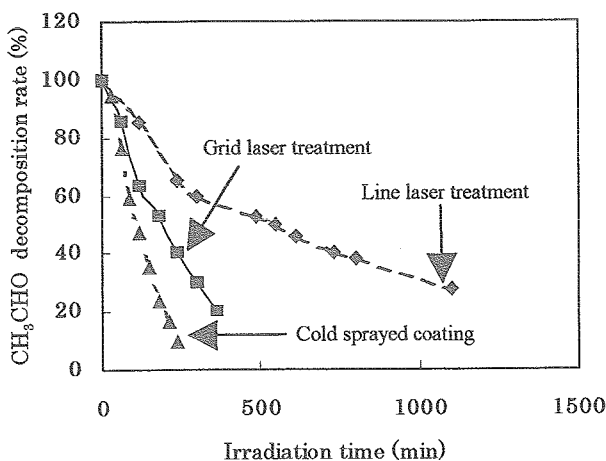


Fig.7 Decay characteristics of acetaldehyde concentration with TiO₂-Zn coatings

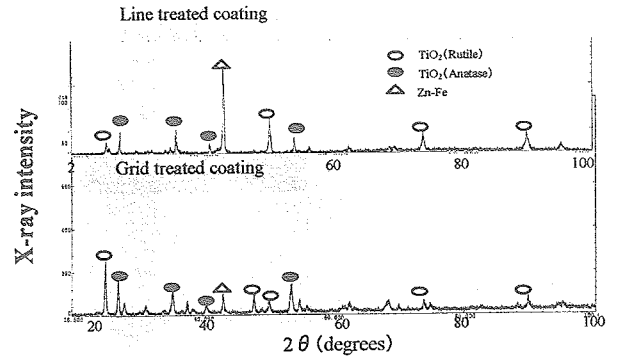


Fig. 8 XRD pattern of laser treated TiO₂-Zn coatings

3.3 Properties of laser treated TiO₂-ZrO₂-WC-Co coatings

The results of SEM images of the surface of as sprayed coatings and laser-treated TiO₂-ZrO₂-WC-Co coatings are shown in Fig.9. The laser treated TiO₂-ZrO₂-WC-Co coatings became denser and smoother than those of cold spraying. Figure 10 shows SEM and EPMA images of the cross section of TiO₂-ZrO₂-WC-Co coatings after laser treatment at a power of 150W and a scan-speed of 8 mm/sec. WC, Co and Zr were distributed uniformly. A diffusion zone at the interface is seen after laser treatments. The uniformly sealed depth of layer was obtained over the whole area of the sample treated by the diode laser.

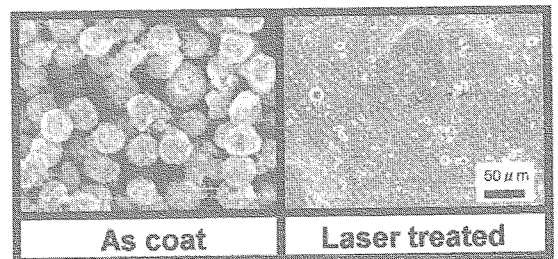


Fig.9 SEM images of as coat and laser treated TiO₂-ZrO₂-WC-Co coating

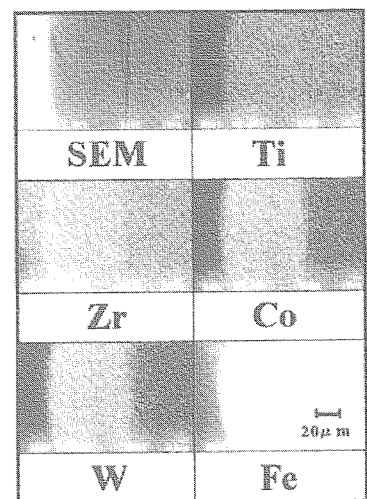


Fig.10 EPMA analysis of laser treated TiO₂-ZrO₂-WC-Co layer

Surface Modification of $\text{TiO}_2\text{-ZrO}_2$ Layers with Direct Diode Laser

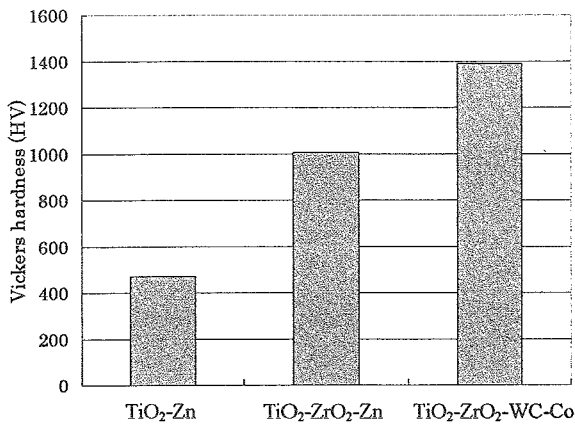


Fig.11 Microhardness results of laser treated solid cold sprayed composite coatings.

The average microhardnesses of the laser treated coatings are presented in Fig.11. Laser treated $\text{TiO}_2\text{-ZrO}_2\text{-WC-Co}$ coatings have very high microhardness values. It is seen that the Vickers hardness of all the $\text{TiO}_2\text{-ZrO}_2\text{-Zn}$ coatings increases compared with the $\text{TiO}_2\text{-Zn}$ coatings without ZrO_2 powder. The Vickers hardness of the laser treated $\text{TiO}_2\text{-ZrO}_2\text{-WC-Co}$ coatings increased with the content of WC. Very high microhardness values in the range of 1280~1490 HV were measured in the specimens.

4. Conclusions

The results are summarized as follows.

- (1) The laser treated $\text{TiO}_2\text{-Zn}$ composite coatings exhibit a high density and high bond strength. The photocatalytic properties of the grid laser treated $\text{TiO}_2\text{-Zn}$ composite coatings were excellent, being equivalent to those of cold spray $\text{TiO}_2\text{-Zn}$ composite coatings.
- (2) The laser treated $\text{TiO}_2\text{-ZrO}_2\text{-WC-Co}$ coatings showed high microhardness values from 1280 to 1490 VHN_{50} . The laser treatment was found to improve the particle bond strength and density at the optimum conditions of the laser power and scan speed.
- (3) The Vickers hardness of the laser treated $\text{TiO}_2\text{-ZrO}_2\text{-Zn}$ composite coatings increased with the ZrO_2 content.

References

- 1) Robert.B.Heimann; Plasma-Spray Coating, VCH, p22 (1996)
- 2) J.Morimoto, A.Yamaguchi, Y.Arata; Proceedings of the 12th International Thermal Spray Conference, p.39 (1989)
- 3) T.Stoltenhoff, H.Kreye, H.J.Richter, H.Assadi; Proceedings of the International Thermal Spray Conference (ASM), p.409, (2001)
- 4) J.Vicek, H.Huber, H.Voggenreiter, A.Fischer, H.Hallen; Proceedings of the International Thermal Spray Conference (ASM), p.417, (2001)